








FULL PAPER

Titanium (IV) complexes of some tetra-dentate symmetrical bis-Schiff bases of 1,6-hexanediamine: Synthesis, characterization, and in silico prediction of potential inhibitor against coronavirus (SARS-CoV-2)

Mohammad Nasir Uddin¹  | Md. Shaharier Amin¹  | Md. Saifur Rahman¹  |
Sonia Khandaker¹  | Wahhida Shumi²  | Md. Atiar Rahman³  |
Sheikh Mahbubur Rahman⁴ 

¹Department of Chemistry, University of Chittagong, Chittagong, Bangladesh

²Department of Microbiology, University of Chittagong, Chittagong, Bangladesh

³Department of Biochemistry & Molecular Biology, University of Chittagong, Chittagong, Bangladesh

⁴UL Laboratories, Dhaka, Bangladesh

Correspondence

Mohammad Nasir Uddin, Department of Chemistry, University of Chittagong, Chittagong, Bangladesh.

Email: nasircu72@gmail.com;
mnuchem@cu.ac.bd

Symmetrical bis-Schiff bases (LH_2) have been synthesized by the condensation of 1,6-hexanediamine (hn) and carbonyl or dicarbonyl. One of the synthesized Schiff bases has been subjected to the molecular docking for the prediction of their potentiality against coronavirus (SARS-CoV-2). Molecular docking revealed that tested Schiff base possessed high binding affinity with the receptor protein of SARS CoV-2 compared with hydroxychloroquine (HCQ). The ADMET analysis showed that ligand is non-carcinogenic and less toxic than standard HCQ. Schiff bases acting as dibasic tetra-dentate ligands formed titanium (IV) complexes of the type $[TiL(H_2O)_2Cl_2]$ or $[TiL(H_2O)_2]Cl_2$ being coordinated through ONNO donor atoms. Ligands and complexes were characterized by the elemental analysis and physicochemical and spectroscopic data including FTIR, 1H NMR, mass spectra, UV-Visible spectra, molar conductance, and magnetic measurement. Optimized structures obtained from quantum chemical calculations supported the formation of complexes. Antibacterial, antifungal, and anti-oxidant activity assessments have been studied for synthesized ligands and complexes.

KEYWORDS

anti-oxidant activity, bis-Schiff bases, coronavirus (SARS-CoV-2), inhibitors, titanium (IV) complexes

1 | INTRODUCTION

A new infectious disease affected millions of people throughout the world that is caused by severe acute respiratory syndrome coronavirus-2 (SARS-CoV-2). It has recently been declared as a pandemic by the World Health Organization.^[1] It is a challenging process though vital to discover fruitful drugs against SARS-CoV-2. Having no alternatives, favipiravir,

remdesivir, chloroquine, and hydroxychloroquine that are previously designed antiviral drugs are recommended in some countries though still they are under investigation by the US Food and Drug Administration as a treatment for COVID-19.^[2]

Schiff bases containing azomethine group $>C=N-$ show broad range of applications in medicine due to their pharmacological properties.^[3] The $>C=N-$ linkage in azomethine derivatives is essential for biological

activity.^[4–7] Several azomethines were reported to possess remarkable antimicrobial, anticancer, and diuretic activities.^[8] Antiviral property of Schiff bases was reported by Chaturvedi and Kamboj.^[9] Antiviral activities of Schiff base prepared from isatin against moloney leukemia virus, vaccinia, rhino virus, and SARS virus have been reported.^[10]

Structures, stereochemistry, and mechanism of the formation of the Schiff base complexes and their analogues have been reviewed.^[11] Tetra dentate Schiff base ligands are synthesized by the condensation of β -diketones or *o*-hydroxyaldehydes or ketones with diamines.^[12] The antimicrobial activity of nine Ln (III) complexes of the Schiff base ligand derived by the condensation of 2-hydroxy-1-naphthaldehyde with 1,6-hexanediamine was explored by Ajlouni et al.^[13] Bayoumi and his co-workers^[14] synthesized and characterized several hexamethylenediamine-metal complexes showing octahedral geometry. Despite the potential of the Schiff base ligands, there has been comparatively only a few works done using titanium (IV) ion. Coordination chemistry of titanium dominated by 4+ oxidation state is either achieved in the form of oxo-titanium (IV), TiO^{2+} or in the form of non-oxotitanium (IV), Ti^{4+} ion when all electrons of valence are lost. Jiling Huang et al. reported the synthesis of two kinds of titanium (IV) complexes with Schiff base as the mixed ligands.^[15] Uddin et al. prepared and characterized the titanium (IV) complexes of the unsymmetrical Schiff base ligands of ethylenediamine and salicylaldehyde, *o*-hydroxyacetophenone, and *o*-hydroxynaphthaldehyde when unsymmetrical ligands are synthesized through in situ partial displacement of the symmetrical bis-Schiff bases.^[12]

The number of the pure coordination compounds, especially the chelate compounds with non-oxotitaniumTi (IV), is limited. This research has been designed to study some chemical behavior of titanium (IV) through the formation of complexes of tetradentate Schiff bases prepared from 1,6-hexanediamine with different aldehydes/ketones, expected to have either six-coordinated octahedral or eight-coordinated unusual geometry with non-oxotitanium (IV). Prepared Schiff bases and titanium (IV) complexes were characterized with the evidence of ^1H NMR, FTIR, UV-Visible and mass spectra, magnetic and conducting behavior, and quantum chemical calculations. Antibacterial, antifungal, and anti-oxidant activity of the prepared ligands and complexes also has been assessed. In context to the recent demands molecular docking approach has been applied for screening of a Schiff base as potent inhibitor of SARS-CoV-2 main protease (PDBID: 6Y84).

2 | METHODS AND MATERIALS

2.1 | Chemicals

All chemicals used in these analyses were of analytical grade and used as procured. 1,6-hexanediamine (hn), 2-hydroxyacetophenone (HAP), 2-hydroxynaphthaldehyde (HNP), and ethyl acetoacetate (EAA) (purity 99.50%) were from Aldrich Chemical, Germany. Salicylaldehyde (Sal) (purity 99.00%) from Riedel-de-Haen, acetylacetone (AA) (purity 99.50%) from Merck, Germany, and succinic acid (SA) (purity 99.00%) from Sigma, Germany, were collected. All necessary precautions were taken to exclude moisture and oxygen during the synthesis and handling of the compounds. The solvents (DMSO, DMF, MeOH, and EtOH) were analytically graded and further purified by using standard procedures. $\text{TiCl}_4 \cdot 6\text{H}_2\text{O}$ (purity 99.50%) was used for the synthesis of Schiff base complexes of V (IV).

2.2 | Synthesis of Schiff bases

Solid 1,6-hexanediamine (hn; 20 mmol) was dissolved in 50 ml of methanol. To which methanolic solution of 40 mmol (1:2 ratio) of aldehyde/ketones (salicylaldehyde-Sal, 2-hydroxy-1-naphthaldehyde-HNP, acetylacetone-AA, 2-hydroxyacetophenone-HAP, 2-hydroxy propiophenone-HPP, and ethylacetoacetate-EAA) was added drop wise with continuous stirring, and the mixture was heated to reflux for 2 h. After completion of the reflux, the dense mixture was transferred in a 150 ml beaker and allowed to cool at room temperature. After cooling, product mixture was kept at a dry place for 24 h at a temperature near about 15°C when colored solid product was seen clearly. This was then filtered off, washed with methanol, dried, and preserved in the desiccator over silica gel along with calcium chloride. Figure 1 shows the schematic presentation of synthesis of a representative ligand, Sal-hn-SalH_2 . Prepared Schiff bases are bis(salicylaldehyde)hexanediamine, Sal-hn-SalH_2 (yellowish, yield 75%, mp 76°C); bis(2-hydroxy-1-naphthaldehyde)hexanediamine, HNP-hn-HNPH_2 (greenish, yield 90%, mp 164°C); bis(acetylacetone)hexanediamine, AA-hn-AAH_2 (reddish, yield 85%, mp 78°C); bis(2-hydroxyacetophenone)hexanediamine, HAP-hn-HAPH_2 (greenish yellow, yield 90%, mp 88°C); bis(2-hydroxypropiophenone)hexanediamine, HPP-hn-HPPH_2 (yellowish, yield 90%, mp 110°C); bis(ethylacetoacetate)hexanediamine, EAA-hn-EAAH_2 (light brownish, yield 65%, mp 68°C).

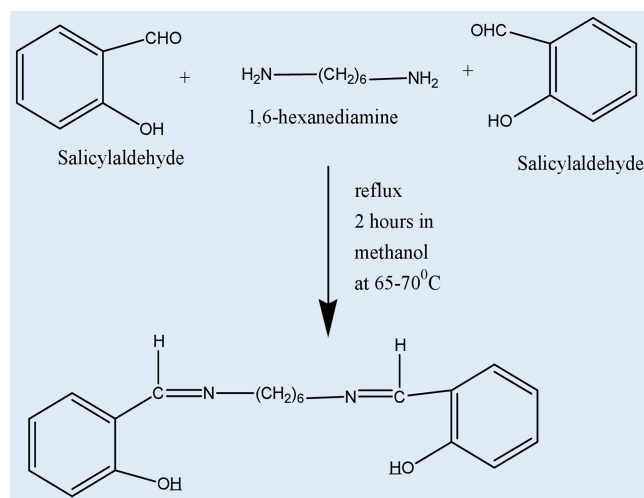


FIGURE 1 Schematic presentation of synthesis of a representative ligand, Sal-hn-SalH₂

2.3 | Synthesis of Ti (IV) complexes

A colorless solution of TiCl₄·6H₂O (10 mmol) in ethanol was added gradually drop wise with continuous stirring to a solution of ligands (10 mmol) in ethanol at room temperature. The reaction mixture was heated to reflux for 2.5 h. After completion of the reflux, the dense mixture was transferred in a beaker and allowed to cool at room temperature and then carefully wrapped with clean, sterile soft paper and kept at a dry place for 48 h at a temperature of about 15°C when the product was seen clearly. This was then filtered off, washed with ethanol, dried, and preserved in the desiccator. Solid complexes were dry and amorphous. Prepared complexes are **C1**-Ti[(Sal-hn-Sal)(H₂O)₂Cl₂] (light pink, yield 55%, mp >200°C); **C2**-Ti[(HNP-hn-HNP)(H₂O)₂Cl₂] (deep brownish, yield 75%, mp >200°C); **C3**-Ti[(AA-hn-AA)(H₂O)₂]Cl₂ (pale brownish, yield 70%, mp >200°C); **C4**-Ti[(HAP-hn-HAP)(H₂O)₂]Cl₂ (yellowish orange, yield 60%, mp >200°C); **C5**-Ti[(HPP-hn-HPP)(H₂O)₂]Cl₂ (orange, yield 60%, mp >200°C); **C6**-Ti[(EAA-hn-EAA)(H₂O)₂]Cl₂ (whitish orange, yield 55%, mp >200°C).

2.4 | Characterization techniques

The following physical and spectral methods, for example, solubility, melting point, infrared, UV-Visible, mass and ¹H NMR spectroscopy, molar conductivity, and magnetic susceptibility measurements were investigated for the characterization of the ligands and complexes. Elemental analytical data and quantum mechanical calculations also applied for these purposes.

2.4.1 | Chemical analysis

Identification of chloride

About 2 g of solid sample was taken in a 25 ml volumetric flask and concentrated. Concentrated HNO₃ was added to digest organic portion of the sample complex, then heated. The mixture was kept about 30 min. The presence of chloride ion in complexes has been identified by both dry and wet tests.^[16]

Quantitative estimation of titanium

Metal estimation is important to decide the geometry and structure of Schiff base complexes. Complexes were brought into solution by decomposing the complexes with concentrated HNO₃ acid followed by evaporation to dryness, and metal content was estimated spectrophotometrically. A standard calibration curve was made using TiO₂ as the source to Ti⁴⁺ according to the standard procedure.^[16] The calibration equation $y = 624.26x + 0.0053$ obtained with $R^2 = 0.9999$ was used to find the titanium concentrations of unknown solutions.

Instrumental analysis

Electronic absorption spectra were run on Shimadzu UV-Visible recording spectrophotometer (Model-1800) using 1 cm cell, and magnetic susceptibility of Ti (IV) complexes was measured with magnetic susceptibility (Balance, Sherwood Scientific, Cambridge, UK) at room temperature at advanced research laboratory, Department of Chemistry, University of Chittagong, Bangladesh. ¹H NMR of Schiff bases and complexes were recorded by Bruker NMR spectrometer from WazedMiah Science Research Center (WMSRC), Jahangirnagar University, Savar, Dhaka, Bangladesh, by dissolving samples in CDCl₃ or DMSO, respectively. Mass spectrum of Schiff bases and their Ti (IV) complexes were recorded by the process “MS Scan” through “Agilent 6460 Triple Quad LC/MS” by dissolving in CDCl₃ or DMSO, respectively. Conductivity measurement was performed on a Hanna conductivity meter (Model-HI 8820 N) dissolving complexes (of the order of 10⁻³ M) in dimethylsulfoxide (DMSO) at 25°C.

2.5 | Computational details

2.5.1 | Quantum chemical calculations by Gaussian 09

Quantum mechanical (QM) methods allow us to calculate different types of energies precisely and interpret various types of complicated interaction between ligands and metal in the formation of complexes. In the present

work, density functional theory with Becke's and exchange functional combining Lee, Yang, and Pare's correlation functional^[17] in Gaussian 09 program package was used for complexes.^[18] PBEPBE/SDD basis set has been employed to optimize the complexes to elucidate their thermodynamic properties such as thermal energy, enthalpy, Gibb's free energy, entropy, dipole moment, and their electronic properties, for example, frontier molecular orbital features (HOMO, LUMO, and HOMO-LUMO gap), hardness, and softness.^[19] The following equations are used to calculate the hardness (η) and softness (S); hardness = [LUMO-HOMO]/2; softness = 1/hardness.

2.5.2 | Preparation of receptor protein

The crystal structure (3D) of COVID-19 Mpro (PDB ID: 6LU7) was collected from online protein data bank (PDB) and used as receptor protein.^[20] The water molecules, hetero atoms, and unwanted molecules were removed from chain A of receptor protein by PyMol (version 2.2) software package^[21] and saved in pdb format. Swiss-Pdb Viewer software (version 4.1.0)^[22] was used to implement for energy minimization of protein. Finally, the protein was ready for molecular docking with optimized molecules considering molecule as ligand and protein as macromolecule.

2.5.3 | Molecular docking simulation, analysis, and visualization

In computer-aided drug design, molecular docking simulation helps to predict binding affinity and mode(s) of ligand and protein.^[23] Molecular docking was performed utilizing PyRx software (version 0.8),^[24] and all rotatable bonds were transferred to non-rotatable involving center gird box size 26.290, 12.6046, and 58.9551 Å along with x , y , and z direction, respectively. Accelrys Discovery Studio (version 4.5)^[25] was utilized to perform non-bonding interactions.

2.5.4 | ADMET analysis

ADMET is important to analyze the pharmacodynamics of the proposed molecules which could be used as drugs. AdmetSAR online database was used to predict the absorption, distribution, metabolism, excretion, and toxicity.^[26] Utilizing both structure data file) and simplified molecular-input line entry system strings, the result was analyzed.

2.6 | Biomedical assessments

Selected Ti (IV) complexes, (**S1**) Ti[(AA-hn-AA)(H₂O)₂]Cl₂, (**S2**) Ti[(HNP-hn-HNP)(H₂O)₂]Cl₂, (**S3**) Ti[Sal-hn-Sal](H₂O)₂Cl₂, (**S4**) Ti[(HPP-hn-HPP)(H₂O)₂Cl₂] prepared from Schiff bases (**S5**) AA-hn-AAH₂, (**S6**) Sal-hn-SalH₂, (**S7**) HNP-hn-HNPH₂, (**S8**) HPP-hn-HPPH₂, respectively, were subjected to evaluate their biomedical assessments, for example, anti-bacterial and anti-fungal activity and antioxidant property. Three human pathogenic bacteria, *Bacillus cereus*, *Salmonella paratyphi*, and *Staphylococcus aureus*, and three fungi, *Aspergillus niger*, *Penicillium sp.*, and *Candida albicans* were collected from the microbiology laboratory, Department of Microbiology, University of Chittagong, Bangladesh.

2.6.1 | Bacterial activity assessment

The "liquid culture method"^[27] was applied for the detection of antibacterial activities. Preparation of nutrient ager (NA) medium, stock culture, preservation of stock culture, and preparation of bacterial suspension were performed according to the procedure stated in literature.^[27]

In this method, 10 ml of liquid NA was taken in each of the test tubes first. Then it was sterilized in autoclave for 15 min. Then different concentration of test samples (0.1%, 0.05%, and 0.01%) was taken at different amount ratio (25, 50, 75, and 100 μ l) in different test tubes. After that 100 μ l of bacterial suspension was taken in each test tubes, and this mixture was thoroughly mixed with continuous shaking. After a while, it was kept in the incubator at temperature near 35°C, and absorbance readings were taken at 600 nm after 3, 6, and 24 h with UV-Visible spectrophotometer using 1 cm cell. All the absorbance readings were taken at least three times ($n = 3$). Mean value and standard deviation of absorbance were taken into account. During recording, absorbance after 24 h saline water was added with the mixture to prevent over growth of bacterial species. During each interval (3, 6, and 24 h) of incubation, the mixture was centrifuged, and the absorbance was taken of the clear supernatant.

2.6.2 | Fungal activity assessment

The anti-fungal activity of the test complexes was studied using PDA as basal medium.^[28] DMSO was used as solvent to prepare desired solution (0.1%) of the test compounds. Proper control was maintained with DMSO in each case of fungi. Potato dextrose agar (PDA) medium

was used throughout the study for the growth and maintenance of fungi. Test tube slants of PDA medium were prepared for the maintenance of cultures. Preparation of liquid potato dextrose medium, stock culture, preservation of stock culture, and preparation of fungal suspension were performed according to the procedure stated in literature.^[28]

At first, 20 ml of sterilized “liquid potato dextrose” medium was taken in 50 ml conical flasks. Ten conical flasks were prepared for one batch of fungus in the same manner. Then 200 μ l of chemical control (DMSO) and different samples were added in each separate conical flask and shaken well to mix thoroughly. A conical flask was kept without chemical control (DMSO) or test samples considered as blank for identifying general growth of each fungus in “liquid potato dextrose” medium. After that, the fungal inoculums (6 mm mycelial block) were placed carefully at each of 10 conical flasks. Initial pH of one batch (chemical control and test samples) was taken before 3 days. All the conical flasks were incubated at room temperature on the laboratory desk for 3 days. After 3 days, growth of fungus in each conical flask was observed, and then it was filtered. The filtrate was used for the pH measurement. Data found were analyzed to understand the change in pH and to establish a correlation between pH change of the culture medium and the fungal inhibition/inducing activity of test samples. The biomass collected after filtration was kept in the oven at 120–150°C to make it dry, and then weight of dry mass of each conical flask was measured.

2.6.3 | Anti-oxidant activity assessment

Selected Schiff base ligands and Ti (IV) complexes were used as test chemicals to justify whether these have good anti-oxidant property or not. Then four experiments were done to evaluate the anti-oxidant property of test samples.

1. Total phenolic content determination (TPC): Total phenolic content of different fraction was determined by a method established by Singleton and Rossi^[29] with some modification.
2. Total anti-oxidant capacity (TAC): The antioxidant activity was evaluated by the phosphomolybdenum method according to the procedure described by Prieto et al.^[30]
3. DPPH free radical scavenging activity: DPPH (2,2-diphenyl-1-picrylhydrazyl) radical scavenging assay was done by Hatano et al.^[31]
4. Hydroxyl radical scavenging activity: It is commonly used to evaluate the free radical scavenging

effectiveness of various antioxidant substances according to Kalidas et al.^[32] with slight modification.

3 | RESULTS AND DISCUSSION

3.1 | Characterization of ligands

These prepared ligands were characterized by melting point determination, solubility test, UV-Visible, FTIR, ¹H NMR, mass spectra, and quantum chemical calculations. All ligands are insoluble in methanol or ethanol but soluble in CHCl₃ in cold. Though all are soluble in DMSO, acetone, and DMF on heat, Sal-hn-SalH₂ is soluble in cold in DMSO. Sharp melting points of all ligands have been recorded. Elemental analysis (% C, H) results support their formation (Table S1).

The infrared spectra of the Schiff bases were recorded using KBr disc in the range of 500–4000 cm⁻¹, and data are presented in Table S1. The important features observed in the infrared spectra of the prepared Schiff base ligands are a weak broad band around 3368–3422 cm⁻¹ indicating the presence of (—OH) group in hydrogen bonding.^[33,34] The present Schiff base ligands contain the ν C=N modes showing its characteristic sharp band at 1558–1655 cm⁻¹. On the basis of various studies, bands observed in the region of ~1562–1620, 1242–1400, 1130–1134, and 1500–1510 cm⁻¹ have been assigned due to ν C—N, ν C—C, ν C—O, and ν C=C, respectively.^[33,34] The bands observed at 1130–1134 cm⁻¹ were assigned to the stretching frequency of the phenolic ν (C—O). Bands observed at ~3048–3178 cm⁻¹ were assigned to the presence of aromatic stretching of the C—H bond. Furthermore, the presence of bands at ~2862–2889 and 2927–2940 cm⁻¹ were assigned to the presence of both symmetric and asymmetric stretching of C—H bonds in both alkyl and phenyl environment of the ligands. The presence of bands in the region of ~630–791, ~864–924, and ~1315–1585 cm⁻¹ is assigned for the presence of —CH₂— bonds ν (—CH₂—), out of plane deformation of —CH₂— bonds.^[35]

The UV-Visible spectra of the Schiff base ligands were recorded in DMSO solution. All the ligands have showed the electronic spectral absorption in the region of near ultraviolet between 200 and 400 nm. These spectra are reproduced in Table S1. UV-Visible spectra of the ligands at a range of 252–315 nm and 330–406 nm are attributed to the π - π^* (benzoid and azomethine) and n- π^* (azomethine) transition, respectively.^[36,37]

The ¹H NMR spectral data of the free ligands recorded in CDCl₃ against tetramethylsilane (TMS) as internal reference is presented in Table S1. The ¹H NMR of the prepared Schiff base ligands had shown signals for

methyl protons, methylene protons, aromatic protons, and hydroxyl and azomethine protons. The ^1H NMR spectra of AA-hn-AAH₂ and EAA-hn-EAAH₂ displayed the R—OH protons and ethylene proton (—C=CH) protons at 12.01–12.70 and 3.75–4.17 ppm, respectively. The ^1H NMR spectra of Sal-hn-SalH₂, HNP-hn-HNPH₂, HPP-hn-HPPH₂, and HAP-hn-HAPH₂ displayed the phenolic O—H protons at 12.37–14.40 ppm. Azomethine protons (—N=CH) in Sal-hn-SalH₂ and HNP-hn-HNPH₂ appeared at 8.54–8.85 ppm.^[13,38] The signals due to methyl protons were observed at 1.21–1.83 ppm, and the methylene protons were observed between 1.56 and 3.72 ppm for all ligands.^[13,14,38] In most of the cases, both methyl and methylene protons interfered each other. Figure 2 presents the ^1H NMR spectrum of a representative ligand, Sal-hn-SalH₂.

The mass spectra of the free ligands confirmed the proposed formula of ligands by showing a series of peak at different mass-to-charge (m/z) ratios. DMSO was used as the dissolving media for sample.^[13,39] Molecular ion peaks (m/z) of all ligands are tabulated in Table S1. The mass fragmentation pattern of HNP-hn-HNPH₂ ligand is depicted in Figure 3. Mass spectral evidence of “HNP-hn-HNPH₂” ligand had shown the fragmentation pattern in the (m/z ratio) range 425.20–152.30. Slight deviation m/z of molecular ion peak may be due to spectrum handling or monitoring error or may be due to the presence of impurities or may be due to isotopic abundance of

hydrogen in the sample produced due to higher ionization potential or some other reasons.

It was observed that all ligands were insoluble in methanol, a solvent used for the preparation of ligands confirming their successful formation. Major IR spectral band such as $\nu\text{C}=\text{N}$ was found in the range of 1558–1655 cm^{-1} . Also, a broad peak in the range of 3368–3422 cm^{-1} had confirmed the presence of $\nu(\text{—OH})$ in the ligand structure, indicating that (—OH) group is present in ortho position. Electronic spectral evidences had ensured the occurrence of $\pi\text{—}\pi^*$ and $\text{n—}\pi^*$ transitions for the ligands. Evidences from ^1H NMR spectroscopy had suggested the proper presence of δCH_2 , δCH_3 , $\delta(\text{C}=\text{N})$, and $\delta(\text{—OH})$ spectral peak in relatively proper ppm range. Mass spectral evidences of ligands had shown relatively correct fragmentation pattern that comply with their molecular mass. All these spectral evidences and elemental analysis date ensured the formation of desired ligands.

3.2 | Characterization of complexes

3.2.1 | Physico-chemical analysis

All the prepared complexes were quite hygroscopic in nature. So these were transferred to dry desiccator as early as possible after synthesis. Also, sweet aroma was

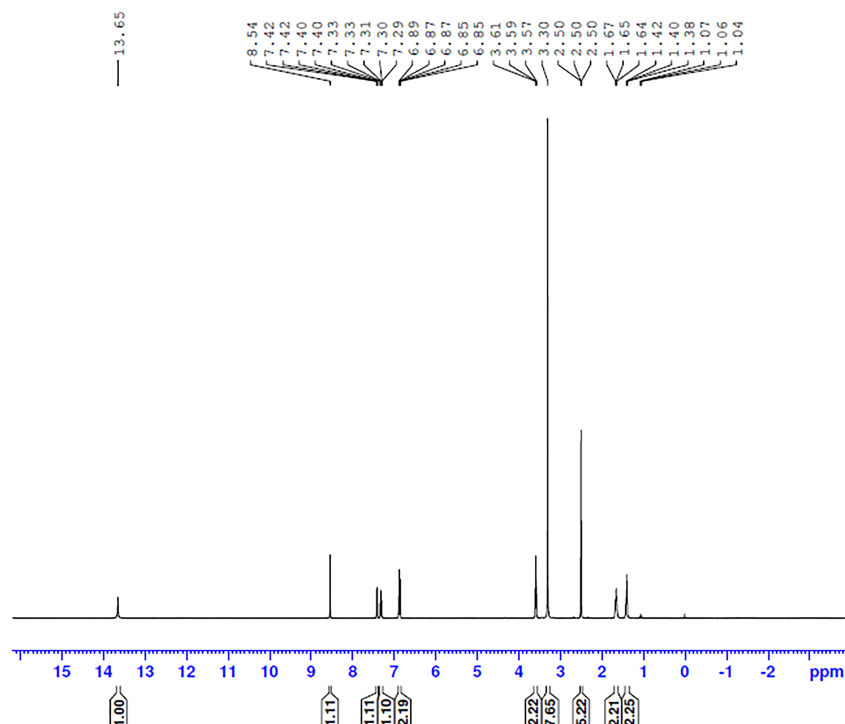
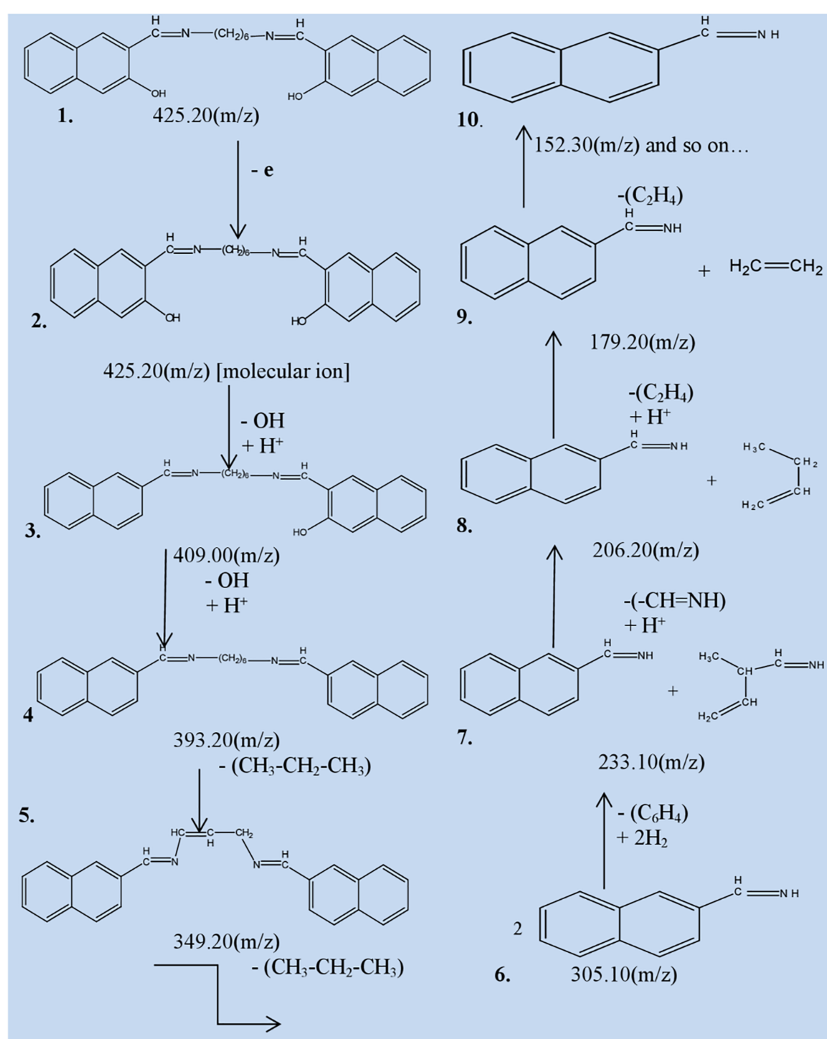


FIGURE 2 ^1H NMR spectrum of a representative ligand, Sal-hn-SalH₂

FIGURE 3 Mass fragmentation pattern of HNP-hn-HNPH₂



found during condensation and storing, whereas prepared ligands had bitter scent or nothing at all. It is seen that there is a clear difference between the melting point of prepared ligands and complexes that confirms their successful formation. Melting points of all complexes exceeded 200°C, which are higher than their respective ligands. All complexes are mostly insoluble in ethanol and in methanol used as solvent in their synthesis. In acetone, CHCl₃ and DMF complexes are insoluble or partially soluble. In DMSO, all are soluble on heat. At the mouth of a test tube glass rod soaked with concentrated NH₄OH created white fume, indicating the presence of chloride in all complexes in qualitative identification. It was also confirmed by wet test for qualitative chloride identification. In case of complexes, Ti[(Sal-hn-Sal)(H₂O)₂Cl₂] and Ti[(HNP-hn-HNP)(H₂O)₂Cl₂], formed white curd like ppt. were less dense compared with other complexes such as Ti[(AA-hn-AA)(H₂O)₂Cl₂], Ti[(HAP-hn-HAP)(H₂O)₂Cl₂], Ti[(HPP-hn-HPP)(H₂O)₂Cl₂] and Ti[(EAA-hn-EAA)(H₂O)₂Cl₂]. From this particular test, it

was seen that chloride ion might be present at the outer sphere in the Ti (IV) complexes.

3.2.2 | Infrared spectra

The infrared spectra of the Ti (IV) complexes were recorded using KBr disc in the range of 400–4000 cm⁻¹, and data are presented in Table S2. A vibrational spectrum provides valuable information regarding the nature of functional group attached to the metal ion in a complex. Attention has been focused on a limited number of bands that provide considerable structural information in order to suggest the most probable manner of coordination of the ligand with the metal atom.^[33] FTIR spectrum of a representative complex, [Ti (Sal-hn-Sal)(H₂O)₂Cl₂] has been presented in Figure 4. The azomethine nitrogen νC=N stretching frequency of the complexes appeared in the range of 1508–1635 cm⁻¹, which is shifted to lower by approximately 20–50 cm⁻¹ than the free ligands.^[13,40]

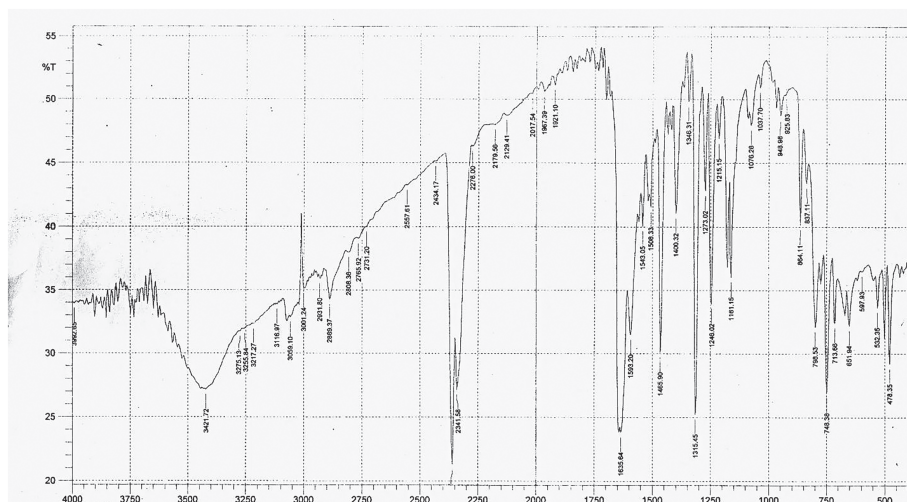


FIGURE 4 FTIR spectrum of a representative complex, $[\text{Ti}(\text{Sal-hn-SalH}_2)(\text{H}_2\text{O})_2\text{Cl}_2]$

These bands are shifted to lower wave numbers indicating the involvement of azomethine nitrogen in coordination to the metal ion.^[34–39] In the complexes, $\nu\text{C}=\text{O}$ frequency was found in the range of $1245\text{--}1292\text{ cm}^{-1}$, which is shifted to higher than free ligands. It is due to the coordination of titanium as confirmed by the presence of $\nu\text{Ti}=\text{O}$ at $370\text{--}451\text{ cm}^{-1}$.^[28] The broad $\nu\text{O}=\text{H}$ band at the range of $3368\text{--}3422\text{ cm}^{-1}$ is absent at the spectrum of complexes, which has been overlapped with H_2O coordination. Bands at $3421\text{--}3468\text{ cm}^{-1}$ due to $\nu\text{O}=\text{H}$ indicates that the central metal is coordinated by water molecule.^[13,40] Coordination sites are further supported by the assignment of $476\text{--}552\text{ cm}^{-1}$ attributed to $\nu\text{Ti}=\text{N}$. Also, appearance of a bond at $370\text{--}421\text{ cm}^{-1}$ attributed to $\text{C}=\text{O}=\text{Ti}$ moiety suggests bonding through phenolic oxygen. The presence of $\nu\text{Ti}=\text{Cl}$ is confirmed by absorption band at 652 cm^{-1} in the complexes, $[\text{Ti}(\text{Sal-hn-Sal})(\text{H}_2\text{O})_2\text{Cl}_2]$ and $[\text{Ti}(\text{HNP-hn-HNP})(\text{H}_2\text{O})_2\text{Cl}_2]$.

3.2.3 | ^1H NMR spectra

The ^1H NMR spectral data presented in Table S2 of the Ti (IV) complexes were recorded in DMSO against TMS as internal reference. The ^1H NMR spectra of the Ti (IV) complexes showed signals for methyl, methylene, ethylene, aromatic, and azomethine protons. The ^1H NMR spectra displayed the aromatic protons at $6.35\text{--}8.53$ (multiplet). Azomethine protons ($-\text{N}=\text{CH}$) generated from aromatic aldehydes showed signals at $8.51\text{--}8.71$ ppm. The ethylene protons ($-\text{C}=\text{CH}$) were observed at $4.01\text{--}4.69$ ppm due to the enolization of diketone upon coordination. The signal due to methyl protons was observed at $1.11\text{--}1.50$ ppm, and the methylene protons were observed between 1.45 and 3.67

(multiplet) ppm. The disappearance of hydroxyl signal and lower shift of azomethyl signals indicates that $\text{O}=\text{H}$ and $-\text{CH}=\text{N}$ groups are involved in chelation.^[13,37,40] Shifting of the bands/peaks in case of complexes than ^1H NMR of ligands (both in lower or higher energy level) indicates that the desired complex formation was successful.

3.2.4 | Electronic spectra

The electronic absorption spectra are often very helpful in the evaluation of results furnished by other methods of structural investigation. The UV-Visible spectra of the Ti (IV) Schiff base complexes were recorded in DMSO solution in the range of $200\text{--}600\text{ nm}$ regions. These spectral bands are tabulated in Table S2. UV-Vis spectra of a representative ligand (red), Sal-hn-SalH_2 and its complex (black), $[\text{Ti}(\text{Sal-hn-Sal})(\text{H}_2\text{O})_2\text{Cl}_2]$ have been presented in Figure S1. Bands around $305\text{--}325\text{ nm}$ is assigned as an $n\text{-}\pi^*$ transition. Also, bands around $368\text{--}423\text{ nm}$ is assigned as LMCT.^[37,39] Observed bands in the range of $226\text{--}261\text{ nm}$ are designated as $\pi\text{-}\pi^*$ type transitions.^[40] The electronic absorption bands due to the $n\text{-}\pi^*$ transition of the non-bonding electrons present on the nitrogen of the azomethine group in the Schiff bases are shifted to the lower energy.^[13,14] From these results, it is said that the imine nitrogen atom appears to be coordinated to the metal ion.^[28] These bands were shifted to a shorter wavelength by chelation, which confirms the complex formation. It was difficult to separate spectral bands that occur in complexes due to LMCT from $n\text{-}\pi^*$ transition bands. Most importantly, the absence of any peak above 500 nm (indicating d-d transition) confirms d^0 state of Ti (IV) complexes.

3.2.5 | Mass spectra

The electron impact mass spectra of the prepared Ti (IV) complexes confirmed the proposed formula by showing a series of peak at different mass-to-charge (m/z) ratios. DMSO was used as the dissolving media for the sample. The molecular ions or parent peaks (m/z) are mentioned in Table S2 for respective complexes. Fragmentation pattern of mass spectra of two complexes is discussed herein. Figure 5 shows the mass spectra of a representative complex, $\text{Ti}[(\text{HNP-hn-HNP})(\text{H}_2\text{O})_2\text{Cl}_2]$. The complex, $\text{Ti}[(\text{HNP-hn-HNP})(\text{H}_2\text{O})_2\text{Cl}_2]$, had shown a peak at 579.00 due to molecular ion (parent peak). The series of peaks in the range of 563.10, 514.20, 487.30, 473.50, 447.50, 365.30, 352.70, 325.311, and 277.10 were corresponding to various fragments, and their intensity gives an idea of the stability of these fragments. The complex, $\text{Ti}[(\text{AA-hn-AA})(\text{H}_2\text{O})_2\text{Cl}_2]$, had shown a peak at 437.20 due to molecular ion (parent peak) instead of 435.33. The series of mass spectral peaks at the range of 425, 409, 387, 349, 302, 289, 274, 244, 230, and 202 were corresponding to various fragments, and their intensity gives an idea of the stability of these fragments. Percent deviation of parent peak was estimated in the range of -0.07 to 0.38 . Slight deviation of parent peak might be due to spectrum handling or monitoring error or may be due to the presence of impurities or may be due to

isotopic abundance of hydrogen, carbon, or titanium in the sample produced due to higher ionization potential or some other reasons.^[28] Mass spectral evidence clearly confirms the six coordinated octahedral structure of both electrolytic and non-electrolytic complexes derived from Schiff bases.

3.2.6 | Molar conductance

Mainly molar conductance values are used in obtaining information about the nature of the complex in solution. The interpretation of the molar conductance study results provides information of possible structures of coordination compounds. Generally, for the transition metal complexes, which are insoluble in aqueous medium, conductance data are obtained in non-aqueous medium. Most useful data are generally obtained in non-aqueous solvents such as nitrobenzene, acetonitrile, acetone, dimethylformamide (DMF), dimethylsulphoxide (DMSO), and chloroform.^[13,39] The conductivity of the prepared Ti (IV) complexes was measured in dimethylsulphoxide. Molar conductance data of prepared Ti (IV) Schiff base complexes are enlisted below in Table S2. From the molar conductance data, it is said that complexes **C1** and **C2** did show molar conductance value of 32 and 11 ($\text{ohm}^{-1} \text{cm}^2 \text{mol}^{-1}$), respectively, which is

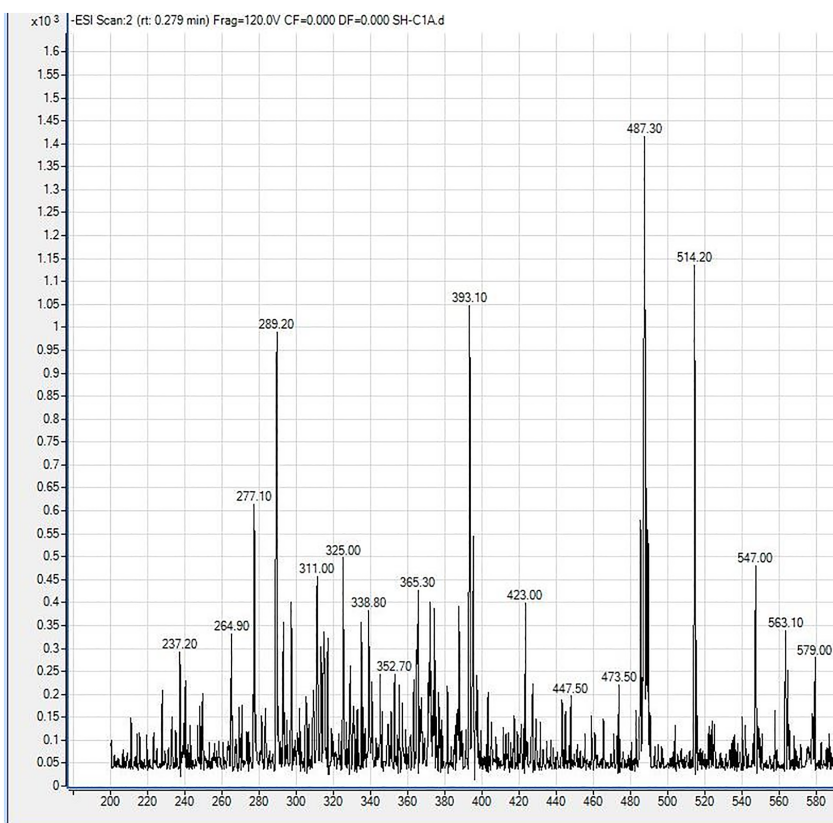


FIGURE 5 The mass spectra of a representative complex, $\text{Ti}[(\text{HNP-hn-HNP})(\text{H}_2\text{O})_2\text{Cl}_2]$

completely different than the remaining complexes having conductance values in the range of 61–97 ($\text{ohm}^{-1} \text{cm}^2 \text{mol}^{-1}$). The values of molar conductance suggested that complexes **C1** and **C2** are non-electrolyte in nature, and the remaining complexes are electrolyte in nature. This is in agreement with the proposed structure for the complexes on the basis of analytical data. Thus, it might be said that complexes derived from Schiff bases of ortho-hydroxyketones or diketones and Ti (IV) complexes (**C3–C6**) are electrolyte in nature, but complexes derived from Schiff bases of ortho-hydroxy aldehydes and their Ti (IV) complexes (**C1** and **C2**) are non-electrolyte in nature.

3.2.7 | Thermal study

Thermal analysis is used to evaluate the stability of the metal complexes and the existence of hydrated or coordinated water molecules. Sharp melting points of complexes could not be detected. Decomposition of complexes is observed at/above 200°C. At this temperature, certain amount of complexes was heated till gaining a constant weight. Calculated mass lost was 7.36%, 6.32%, 8.17%, 6.88%, 6.85%, and 7.43% for C1, C2, C3, C4, C5, and C6, respectively, which are in close agreement with their theoretical mass loss of 7.51%, 6.21%, 8.27%, 7.10%, 6.72%, and 7.27%, respectively. These results comply with the elimination of two coordinated water molecules from complexes.^[5,6]

3.2.8 | Magnetic susceptibility

The magnetic susceptibility of the complexes was found to be in the range of diamagnetic substances. Thus, it can be said that all formed complexes are diamagnetic in nature.^[36,40]

All physic-chemical characteristics data suggested the highest possibility of the formation of Ti (IV) complexes with Schiff bases derived from 1,6-hexanediamine and carbonyl compounds. All chemical and characterization data gave us significant idea about the nature and property of prepared complexes. Two important conclusions can be reached about the geometry of formed complexes from these studies stated above. Mass spectral analysis confirmed the following eight coordinated geometry as Ti[(HNP-hn-HNP)(H₂O)₂Cl₂] and Ti[(Sal-hn-Sal)(H₂O)₂Cl₂]. Molar conductance data supported the non-electrolytic nature of these types of complexes. The electrolytic nature of the remaining complexes, Ti[HAP-hn-HAP)(H₂O)₂Cl₂,

Ti[HPP-hn-HPP)(H₂O)₂Cl₂, and Ti[(AA-hn-AA)(H₂O)₂Cl₂, Ti[(EAA-hn-EAA)(H₂O)₂Cl₂, suggested chloride ions to be outer sphere. 1,6-Hexanediamine possessing two symmetrical amino groups formed bis-Schiff bases with orthohydroxyaldehydes/diketones. Ligands acting as a dibasic tetradentate ligand through ONNO donors satisfy both primary and secondary valencies of Ti (IV) having four donor atoms in a plane. Estimation of Ti⁴⁺ as shown in Table S2 confirms the 1:1 stoichiometry of complexes having evidences that the prepared complexes are mononuclear/monometallic. Along with mass spectral analysis confirmed their geometry as shown in Figure 6.

3.3 | Frontier molecular orbital

All the complexes are designed depending on characterization evident such as UV-Vis, FTIR, ¹HNMR, and mass spectroscopy. Quantum mechanical (QM) methods allow us to calculate different types of energies precisely and interpret various types of complicated interaction between ligands and metal in the formation of complexes. In the present work, density functional theory (DFT) with Becke's and exchange functional combining Lee, Yang, and Pare's correlation functional^[17] in Gaussian 09 program package were used for complexes.^[18] PBEPBE/SDD basis set has been employed to optimize the ligands and complexes to elucidate their thermodynamic properties such as thermal energy, enthalpy, Gibb's free energy, entropy, dipole moment, and their electronic properties, for example, frontier molecular orbital features (HOMO, LUMO, and HOMO-LUMO gap), hardness, and softness.^[19] Thermodynamic properties of HNP-hn-HNPH₂ and Ti [(HNP-hn-HNP)(H₂O)₂Cl₂] obtained by “density functional theory” in Gaussian 09 program package are discussed as representative compounds, and the values of thermodynamic properties are tabulated in Table 1. Hardness and softness of this ligand and its complex were also calculated from the energies of frontier HOMOs and LUMOs considering Parr and Pearson interpretation^[41] of harness in DFT and Koopmans theorem^[42] on the correlation of ionization potential (IP) and electron affinities (EA) with HOMO and LUMO energy. Energy gap between HOMO and LUMO of optimized structures is obtained 7.70285 eV for ligand and 1.9012 eV for complex. Geometry of the complexes proposed on the basis of experimental evidences was confirmed by the optimized structures as shown in Figure 7 obtained by quantum chemical calculation for a representative ligand, HNP-hn-HNPH₂ and its complex, Ti[(HNP-hn-HNP)(H₂O)₂Cl₂].

FIGURE 6 Molecular formula and geometry of prepared complexes

| Formula | Structure |
|--|-----------|
| <p>1. $Ti[(Sal-hn-Sal)(H_2O)_2Cl_2]$,</p> <p>2. $Ti[(HNP-hn-HNP)(H_2O)_2Cl_2]$, Where, R= (fused phenyl).</p> | |
| <p>3. $Ti[(HAP-hn-HAP)(H_2O)_2]Cl_2$, 4. $Ti[(HPP-hn-HPP)(H_2O)_2]Cl_2$ Where, R= (CH₃-, C₂H₅-)</p> | |
| <p>5. $Ti[(AA-hn-AA)(H_2O)_2]Cl_2$</p> <p>6. $Ti[(EAA-hn-EAA)(H_2O)_2]Cl_2$ Where, R= (CH₃-, -OC₂H₅),</p> | |

3.4 | Biomedical assessment results

3.4.1 | Discussion on bacterial activity assessment

Bacterial activity assessment of prepared Ti (IV) complexes (**S1–S4**) of Schiff base ligands (**S5–S8**) did show very low activity against all four tested organisms. Comparison of activity of sample (**S6**) at different concentration and different incubation period against different organism has been shown in Figure S2. In some cases, higher absorbance value was obtained for 75 µl concentration than that of 100 µl concentration. This effect can be said as the minimum amount of concentration that have the ability to enhance aerial growth of bacteria at maximum level which otherwise can be termed as saturation point for test organisms or the optimum chemical used by the organism. Sample **S5** (AA-hn-AA_{H2}) and **S6** (Sal-hn-Sal_{H2}) did show low inhibition activity against

S. paratyphi whereas sample **S7** (HNP-hn-HNP_{H2}) did show stimulating effect against all tested organisms and **S4**, Ti[(HPP-hn-HPP) (H₂O)₂]Cl₂, did show stimulating effect against *C. albicans*. After all, it is said that prepared ligands did show better activity (both stimulating and inhibiting) than prepared Ti complexes of these ligands.

3.4.2 | Discussion of fungal activity of test samples

Fungal activity against Aspergillus niger

The prepared ligands and complexes were tested by liquid media method by measuring pH of the solutions against *Aspergillus niger*. Figure 8 showed that in the presence of test samples, fungal biomass showed lower pH (acidic) except sample **S5** after 3 days incubation. Control species (test organism) in liquid medium tends to be neutral at pH value, whereas chemical control species

TABLE 1 (a.) Thermodynamic properties of HNP-hn-HNPH₂ and Ti[(HNP-hn-HNP)Cl₂].2H₂O obtained by “density functional theory,” (b.) binding affinity, nonbonding interaction, and (c.) pharmacokinetic properties of HNP-Hn-HNPH₂ and hydroxychloroquine with SARS Cov-2

| a. Thermodynamic properties | | | b. Binding affinity, nonbonding interaction | | | | |
|--|--------------------------|--|---|-----------------------------|---------------------|--|--------------|
| Property | HNP-hn-HNPH ₂ | Ti[(HNP-hn-HNP)(H ₂ O) ₂ Cl ₂] | Name | Binding affinity (kcal/mol) | Residues in contact | Interaction type | Distance (Å) |
| Electronic energy (Hartree) | -652.7109 | -1400.953 | HNP-hn-HNPH ₂ | -6.3 | Gln110 | H | 2.4452 |
| Enthalpy (Hartree) | -652.8021 | -1400.952 | | | Gln110 | C | 3.0672 |
| Gibb's free energy (Hartree) | -653.3249 | -1401.031 | | | Phe294 | Pp | 3.8712 |
| Dipole moment (D) | 1.9703 | 7.309 | | | Phe294 | Pp | 3.8836 |
| ² HOMO (eV) | -8.5669 | -5.2115 | HCQ | -5.8 | Tyr154 | H | 2.47092 |
| ² LUMO (eV) | -0.8640 | -3.3103 | | | Gln110 | H | 2.80338 |
| Gap (E _L -E _V) eV | 7.70285 | 1.9012 | | | Thr111 | H | 2.89271 |
| Hardness | 3.8514 | 7.309 | | | Asp153 | C | 2.43213 |
| Softness | 0.2596 | 1.0519 | | | Gln110 | C | 2.56382 |
| | | | | | Thr111 | C | 2.29355 |
| | | | | | Arg298 | A | 3.77516 |
| c. Pharmacokinetic parameters | | | | | | | |
| Drug | Blood brain barrier | Human intestinal absorption | P-glyco protein inhibitor | hERG | Carcinogen | Rat acute toxicity LD ₅₀ (mol/kg) | |
| HNP-hn-HNPH ₂ | +(0.6626) | +(0.9282) | NI(0.7147) | SI(0.6178) | NC(0.8182) | 2.2838 | |
| HCQ | +(0.5602) | +(0.9892) | NI(0.7297) | WI(0.6798) | NC(0.8370) | 2.6348 | |

Abbreviations: A, alkyl; C, carbon hydrogen bond; H, conventional hydrogen bond; NC, non-carcinogen; NI, non-inhibitor; PA, Pi-alkyl; WI, weak inhibitor.

became acidic (after 3 days); however, in the presence of test ligands and complexes, the fungal medium became acidic that means that pH of the sample **S1**, **S2**, **S3**, **S4**, **S6**, and **S7** became 2.30, 2.53, 2.32, 4.74, 5.41, and 4.41, respectively, but in case of **S5**, pH of the sample tends to be less acidic or neutral by showing pH value 6.29. Figure S3 showed that the test sample expressed more or less biomass after 3 days incubation. From the biomass of *Aspergillus niger* species, it is seen that **S4** and **S6** have the inducing capacity to enhance the aerial growth of this species, whereas **S1** and **S2** have similar activity as the control. On the other hand, **S3**, **S5**, and **S7** have the inhibition ability.

Fungal activity against *Penicillium* sp.

The prepared ligands and complexes were tested by liquid media method by measuring pH of the solutions against *Penicillium* sp. The results showed that with the presence of test samples, fungal biomass showed lower

pH (acidic or weak acidic) after 3 days incubation. Control species (test organism) in liquid medium tends to be neutral at pH value, whereas chemical control species became acidic (after 3 days); however, in the presence of test ligands and complexes, the fungal medium became acidic that means that pH of the sample **S1**, **S2**, **S6**, and **S7** became 3.62, 2.88, and 3.90, respectively, and in case of sample **S1**, **S3**, **S4**, and **S5**, pH became less acidic. pH values of sample **S1**, **S3**, **S4**, and **S5** became 5.57, 5.06, 5.40, and 5.42, respectively. The fungal biomass result, which was measured by dry weight measured technique, showed that the test sample expressed more or less biomass after 3 days incubation. From the biomass of *Penicillium* sp., it is seen that sample **S2**, **S4**, **S5**, **S6**, and **S7** have the inducing capacity to enhance the aerial growth of this species, whereas sample **S1** and **S4** have the inhibition ability.

From this study, it can be said that prepared ligands did show better inhibition activity than Ti (IV) complexes

FIGURE 7 Optimized structure, HOMO, and LUMO of HNP-hn-HNPH₂ and Ti[(HNP-hn-HNP)(H₂O)₂Cl₂] after DFT calculations

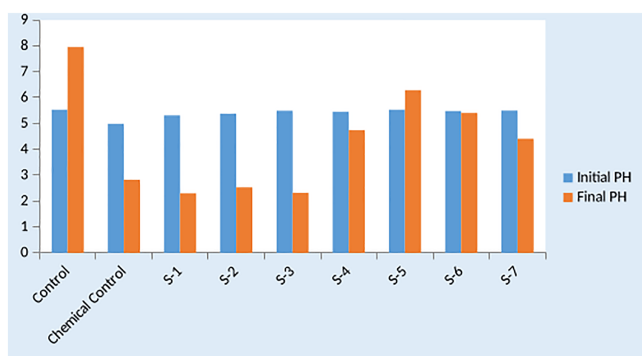
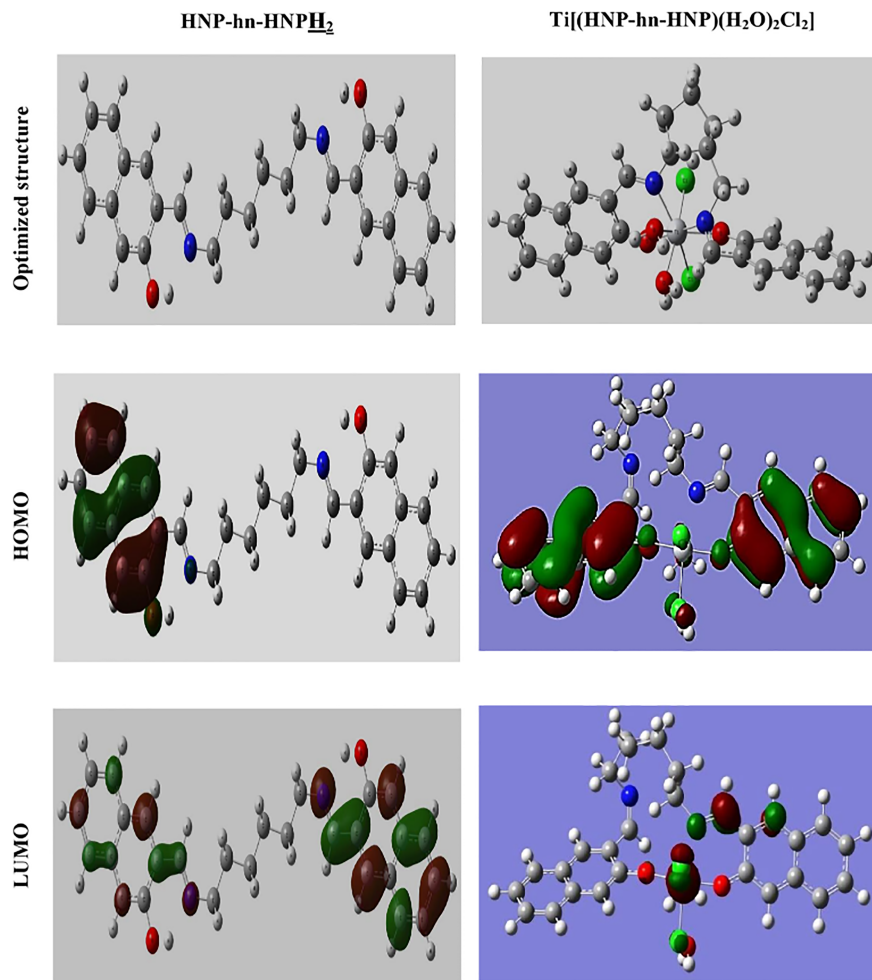


FIGURE 8 Fungal activity evaluation of test samples against *Aspergillusniger* by pH measurement

of respective ligands. Similar results were investigated for oxotitanium (IV) complexes of Schiff bases prepared by the condensation of 2-hydroxy-1-naphthaldehyde with o-phenylenediamine.^[36] It can best be explained by chelation theory that states that the influence of positive charge of metal π -electrons of Schiff bases get delocalized over the whole chelate.^[5,6] It is the chelation that increases lipophilic property of complexes and assists

their permeation through the lipid layer of the cell membranes of microorganisms. But in general, it can be said that prepared ligands and complexes did show stimulating activity, which is supported by lowering of pH value of the liquid medium after certain incubation period (3 days). The titanium (IV) complexes of Schiff bases derived from aroylhydrazine also showed higher inducing capacity against *Salmonella paratyphi* and *Bacillus cereus*.^[28] In case of stimulating activity, it is supposed that microorganisms might consume the ligands by degradation and have their nutrients.

3.5 | In silico studies

3.5.1 | Binding affinity and interactions

In order to find potent SARS-CoV-2 (main protease 6LU7) inhibitor, HNP-Hn-HNPH₂ was selected because Schiff bases are already known to exert antiviral activity against many RNA viruses.^[10] The molecular docking was done to predict the binding affinity and pose of

HNP-Hn-HNPH₂ ligand against SARS-CoV-2 main protease (6LU7). Similarly, hydroxyl chloroquine (HCQ) was docked with same receptor protein as standard (Figure 9). Stronger binding was predicted between ligand and receptor protein through negative value of binding affinity.^[43] The binding affinity of HNP-Hn-HNPH₂ was -6.3 kcal/mol as presented in Table 1. Corresponding value of standard (HCQ) was $-5.8.0$ kcal/mol indicating the higher binding affinity of HNP-Hn-HNPH₂ ligand. This highest binding affinity (-6.3 kcal/mol) of the ligand predicted that it might serve as better inhibitor standard (HCQ). However, ligand is partially located into the receptor protein similar to (HCQ). Hydrogen bond is considered as a significant factor for RNA structure in biological system and less than 2.3 Å increases the binding affinity.^[44] Most significant hydrogen bonds of HNP-Hn-HNPH₂ with Gln110 amino acid residue of protein in a distance 2.4452 was identified which is closer than standard HCQ (Table 1). No significant interaction with the Tyr, Thr catalytic dyad like HCQ was demonstrated for HNP-Hn-HNPH₂. Besides, Pi-Pi hydrophobic interactions with Phe294 and 6LU7 receptor protein was depicted (Figure 10). This special type of Pi-pi stacked interaction with Phe294 is supposed to increase binding affinity in HNP-Hn-HNPH₂-6LU7 complex. Hence, HNP-Hn-HNPH₂-6LU7 complex was stabilized, and HNP-Hn-HNPH₂ was fitted within the substrate binding pocket of 6LU7 Mpro having different binding modes, hydrogen bond interactions, and hydrophobic interactions.

3.5.2 | ADMET analysis

The ADMET predicted that the ligand HNP-Hn-HNPH₂ shows positive response to both blood brain barrier and human intestinal absorption as hydroxychloroquine (HCQ) as shown in Table 1. The ligand was found to be non-carcinogenic and does not inhibit the P-glycoprotein. Therefore, it has protective capacity to interrupt the absorption, permeability, and retention of the drugs.^[45] Ligand along with hydroxychloroquine shows type III acute oral toxicity. Ligand HNP-Hn-HNPH₂ indicates good inhibitor for human ether-a-go-go-related gene (hERG) that can lead to short QT syndrome.^[46]

3.6 | Discussion on anti-oxidant property assessment

The compounds are considered to have antioxidant properties in those that possess biological properties such as antiapoptosis, antiaging, anticarcinogen, antiinflammation, antiatherosclerosis, cardiovascular protection, and improvement of endothelial function, as well as inhibition of angiogenesis and cell proliferation activities.

1. Higher TPC value of any compound indicates higher anti-oxidant property. Method used here to estimate TPC in this research is F-C method, which may suffer from a number of interfering substances. But the proposed geometry suggested for the ligands and complexes suggesting that all the test samples should have

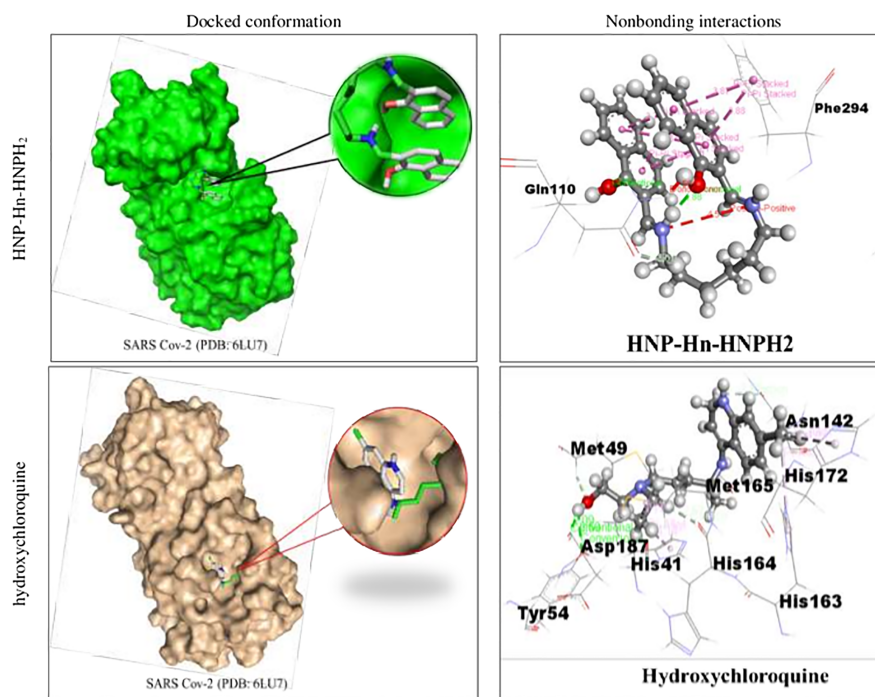


FIGURE 9 Docked conformations and nonbonding interactions of HNP-Hn-HNPH₂ and hydroxychloroquine at inhibition bounding site of receptor protein 6LU7

FIGURE 10 Molecular docking of HNP-Hn-HNPH₂ with receptor protein 6LU7.6LU7-HNP-Hn-HNPH₂ complex depicting the possible hydrogen bonding and hydrophobic Pi-Pi interactions with Gln 110 and Phe 294 amino acid residue, respectively

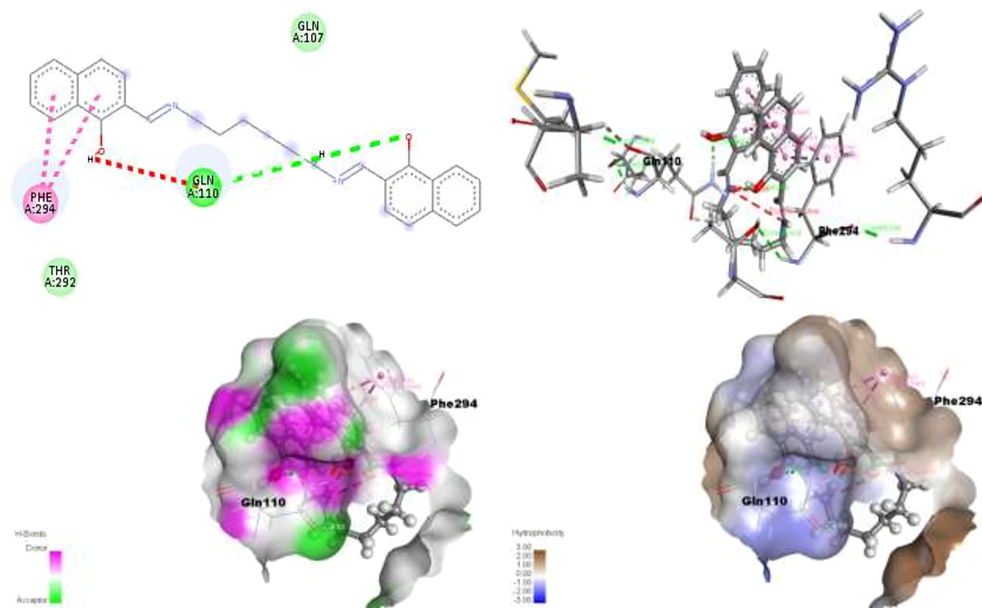


TABLE 2 Total phenolic content and total anti-oxidant capacity of test samples

| Name of test sample | Total phenolic content (mg GAE/g) | | | | Total anti-oxidant capacity (mg AAE/g) | | | |
|--|-----------------------------------|---------------|--------|---------|--|---------------|-------|---------|
| | Eq. conc. (µg/ml) | Average conc. | TPC | RSD (%) | Eq. conc. (µg/ml) | Average conc. | TAC | RSD (%) |
| Ti[(AA-hn-AA)(H ₂ O) ₂] Cl ₂ | 481.28 | 481.09 ± 0.32 | 300.68 | 0.07 | 4.09 | 3.95 ± 0.24 | 4.74 | 5.98 |
| | 481.28 | | | | 4.09 | | | |
| | 480.72 | | | | 3.68 | | | |
| Ti[(HNP-hn-HNP) (H ₂ O) ₂ Cl ₂] | 276.28 | 275.53 ± 0.85 | 172.21 | 0.31 | 9.55 | 9.25 ± 0.53 | 11.56 | 5.68 |
| | 274.60 | | | | 8.64 | | | |
| | 275.72 | | | | 9.55 | | | |
| Ti[(Sal-hn-Sal) (H ₂ O) ₂ Cl ₂] | 135.17 | 134.80 ± 0.32 | 84.25 | 0.24 | 15.00 | 14.15 ± 0.92 | 16.85 | 6.47 |
| | 134.61 | | | | 13.18 | | | |
| | 134.61 | | | | 14.27 | | | |
| Ti[(HPP-hn-HPP) (H ₂ O) ₂ Cl ₂] | 559.61 | 559.24 ± 0.31 | 349.53 | 0.56 | 31.36 | 31.06 ± 0.53 | 38.83 | 1.69 |
| | 559.06 | | | | 30.45 | | | |
| | 559.06 | | | | 31.36 | | | |
| HPP-hn-HPPH ₂ | 109.06 | 109.24 ± 0.85 | 68.28 | 0.77 | 27.73 | 27.43 ± 0.53 | 34.29 | 1.92 |
| | 108.50 | | | | 26.82 | | | |
| | 110.17 | | | | 27.73 | | | |
| AA-hn-AAH ₂ | 93.50 | 93.68 ± 0.85 | 58.55 | 0.90 | | | | |
| | 92.94 | | | | | | | |
| | 94.61 | | | | | | | |
| HNP-hn-HNPH ₂ | 187.38 | 186.64 ± 1.27 | 116.65 | 0.68 | | | | |
| | 187.38 | | | | | | | |
| | 185.17 | | | | | | | |
| Sal-hn-SalH ₂ | 127.39 | 127.02 ± 1.15 | 79.39 | 0.91 | | | | |
| | 125.72 | | | | | | | |
| | 127.94 | | | | | | | |

Abbreviations: TAC, total anti-oxidant capacity; TPC, total phenolic content determination.

higher values of TPC. TPC of samples (S1–S8) suggest that all of these have moderate value as shown in Table 2. But among all of these, S1, S2, S4, and S6 are highly potential as these all have TPC value more than 100 mg GAE/g dry weight. It is decided to say all the test samples (S1, S2, S4, and S6 are prominent among test samples) can show better anti-oxidant property.

- The phosphomolybdate method is quantitative, because total anti-oxidant capacity (TAC) is expressed as ascorbic acid equivalents. In our experiment, TAC values of S4 and S8 are 38.83 ± 0.663 and 34.29 ± 0.663 mg AAE/g dry weights as shown in Table 2, though it is in the range of pro-oxidative property. But due to the presence of water molecule in the structures of S1–S4, it may support the lower value of TAC. Thus, it is decided to say that S2 and S4 are potential for anti-oxidant property by this measurement.
- The DPPH assay is considered to be based on an ET reaction, and hydrogen atom abstraction is a marginal reaction pathway. It is said that the lower the absorbance value of test sample, the higher the DPPH free radical scavenging activity is. Many antioxidants that react quickly with peroxy radicals may react slowly or may even be inert to DPPH due to steric inaccessibility. Higher absorbance value of samples might be due to the presence of color compound or compound with the self-absorbing power. In this DPPH method, the IC_{50} values of sample S4 and S7 and ascorbic acid (standard) are 1.34, 5.25, and 1.77 ($\mu\text{g/ml}$), respectively. The values were highly encouraging as the cut off value of ascorbic acid is 1000. It can be referring to be potential (S4 and S7) as an anti-oxidant agent.
- The hydroxyl radical is an extremely reactive free radical formed in biological system and has been implicated as a highly damaging species in free radical pathology, capable of damaging almost every molecule found in living cell. The hydroxyl radical can cause oxidative damage to DNA, lipids, and proteins. In this method, the IC_{50} values of sample S5, S6, S7, and S8 are 1681.31, 104.77, 3952.65, and 534.20 ($\mu\text{g/ml}$), respectively. Thus, S6 is said to be highly promising among the test samples studied for “hydroxyl radical scavenging activity.”

4 | CONCLUSION

The prepared Schiff bases and their Ti (IV) complexes have been characterized on the basis of physico-chemical and instrumental analysis. Ligands acted as dibasic

tetradentate one coordinated through ONNO donor atoms lying in a plane with respect to metal ion. Stimulating effect was found for sample HNP-hn-HNPH₂ against all studied test organisms (*C. albicans*, *S. paratyphi*, *S. aureus*, and *B. cereus*), whereas AA-hn-AAH₂ and Sal-hn-SalH₂ did show low inhibition activity against *S. paratyphi*. Prepared ligands and complexes did show fungal stimulating activity against *Aspergillus niger* and *Penicillium sp.* Some of the prepared ligands and complexes have potential to be an anti-oxidant agent. The results of molecular docking revealed that HNP-Hn-HNPH₂ have the best binding affinity with the receptor protein compared with the approved medicine, hydroxychloroquine. The ADMET analysis showed that ligand is non-carcinogenic and less toxic than standard HCQ. However, these in silico studies proved that HNP-Hn-HNPH₂ would be a good candidate as inhibitor for SARS-CoV-2. But it is required to perform in vitro and in vivo studies to establish a solid experimental evidence of its activity as inhibitor for COVID-19.

FUNDING

No funding was available.

CONFLICT OF INTEREST

The authors declare that they have no conflict of interest.

AUTHOR CONTRIBUTIONS

Mohammad Nasir Uddin: Conceptualization; methodology; project administration; supervision. **Shaharier Amin:** Formal analysis. **Md. Saifur Rahman:** Software. **Sonia Khandaker:** Formal analysis. **Wahhida Shumi:** Data curation; formal analysis. **Atiar Rahman:** Formal analysis. **Sheikh Mahbubur Rahman:** Resources.

DATA AVAILABILITY STATEMENT

All data and materials are available upon request.

ORCID

Mohammad Nasir Uddin  <https://orcid.org/0000-0003-1235-2081>

Md. Shaharier Amin  <https://orcid.org/0000-0001-7316-2439>

Md. Saifur Rahman  <https://orcid.org/0000-0003-1738-6950>

Sonia Khandaker  <https://orcid.org/0000-0003-4025-6230>

Wahhida Shumi  <https://orcid.org/0000-0001-7593-6792>

Md. Atiar Rahman  <https://orcid.org/0000-0002-4902-8923>

Sheikh Mahbubur Rahman  <https://orcid.org/0000-0002-2230-4932>

REFERENCES

- [1] T. Acter, N. Uddin, J. Das, A. Akhter, T. R. Choudhury, S. Kim, *Sci. Total Environ.* **2020**, 138996.
- [2] T. M. Abd El-Aziz, J. D. Stock, *Infect. Genet. Evol.* **2020**, *83*, 104327.
- [3] R. J. Fessenden, J. S. Fessenden, *Organic chemistry*, Brooks/Cole publishing Company, USA **1998**.
- [4] L. H. Abdel-Rahman, A. M. Abu-Dief, M. Basha, A. A. H. Abdel-Mawgoud, *Appl. Organomet. Chem.* **2017**, *31*(11), e3750.
- [5] L. H. Abdel-Rahman, M. S. Adam, A. M. Abu-Dief, H. Moustafa, M. Basha, A. H. Aboria, B. S. Al-Farhan, H. E. Ahmed, *Appl. Organomet. Chem.* **2018**, *32*, e4527.
- [6] L. H. Abdel-Rahman, A. M. Abu-Dief, M. R. Shehata, F. M. Atlam, A. A. H. Abdel-Mawgoud, *Appl. Organomet. Chem.* **2019**, *33*(4), e4699.
- [7] A. M. Abu-Dief, L. H. Abdel-Rahman, A. A. H. Abdel-Mawgoud, *Appl. Organomet. Chem.* **2020**, *34*(2), e5373.
- [8] H. Schiff, *Justus Liebigs Ann. Chem.* **1864**, *131*(1), 118.
- [9] D. Chaturvedi, M. Kamboj, *Chem. Sci. J.* **2016**, *7*(2).
- [10] L. R. Chen, Y. C. Wang, Y. W. Lin, S. Y. Chou, S. F. Chen, L. T. Liu, Y. T. Wu, C. J. Kuo, T. S. Chen, S. H. Juang, *Bioorg. Med. Chem. Lett.* **2005**, *15*, 3058.
- [11] A. M. Abu-Dief, I. M. A. Mohamed, *Beni-Suef Uni. J. Basic and Appl. Sci.* **2015**, *4*, 119.
- [12] M. N. Uddin, D. A. Chowdhury, K. Hossain, *J. Chin. Chem. Soc.* **2012**, *59*, 1520.
- [13] A. M. Ajlouni, Z. A. Taha, W. Al Momani, A. K. Hijazi, *Inorg. Chim. Acta* **2012**, *388*, 120.
- [14] H. A. Bayoumi, *Characteristics Studies of Hexamethylene Diamine Complexes*, Hindawi Publishing Corporation **2013** 1.
- [15] J. Huang, B. Lian, Y. Qian, W. Zhou, *Macromolecules* **2002**, *35*, 4871.
- [16] A. I. Vogel, *Quantitative Inorganic Analysis*, 4thEdn ed., Longman **1978**.
- [17] C. Lee, W. Yang, R. G. Parr, *Phys. Rev. B* **1988**, *37*, 785.
- [18] M. J. Frisch, G. W. Trucks, H. B. Schlegel, G. E. Scuseria, M. A. Robb, J. R. Cheeseman, *Gaussian 09, Revision A.02*, Gaussian Inc, Wallingford CT 34, Wallingford CT **2009**.
- [19] H. Kruse, L. Goerigk, S. Grimme, *J. Org. Chem.* **2012**, *77*, 10824.
- [20] J. L. Sussman, D. Lin, J. Jiang, N. O. Manning, J. Prilusky, O. Ritter, E. E. Abola, *Acta Crystallogr Sect D Biol Crystallogr.* **1998**, *54*, 1078.
- [21] G. Stockwell, *Biochemistry* **2003**, *42*, 225.
- [22] N. Guex, M. C. Peitsch, *Electrophoresis* **1997**, *18*, 2714.
- [23] M. Uzzaman, M. N. Uddin, *DARU J. Pharm. Sci.* **2019**, *27*, 71. <https://doi.org/10.1007/s40199-019-00243-w>
- [24] S. Dallakyan, A. J. Olson, in *Chemical Biology: Methods and Protocols*, (Eds: J. E. Hempel, C. H. Williams, C. C. Hong), Springer New York, New York, NY **2015** 243.
- [25] Version ADS. **2017**.
- [26] F. Cheng, W. Li, Y. Zhou, J. Shen, Z. Wu, G. Liu, P. W. Lee, Y. Tang, *J. Chem. Inf. Model.* **2012**, *52*, 3099.
- [27] N. K. Ishikawa, M. C. M. Kasuya, M. C. D. Vanetti, *Brazilian J. Micro.* **2001**, *32*, 206.
- [28] M. N. Uddin, S. Khandaker, M. Uzzaman, M. S. Amin, W. Shumi, M. A. Rahman, M. R. Sheikh, *J. Mol. Struct.* **2018**, *1166*, 79e90.
- [29] V. L. Singleton, J. A. Rossi, *Am J EnolVitic.* **1965**, *16*, 144.
- [30] P. Prieto, M. Pineda, M. Aguilar, *Anal. Biochem.* **1999**, *269* (2), 337.
- [31] T. Hatano, H. Kagawa, T. Yasuhara, T. Okuda, *Chem. Pharm. Bull.* **1988**, *36*, 1090.
- [32] S. Kalidas, C. Sanders, X. Ye, T. Strauss, M. Kuhn, Q. Liu, D. P. Smith, *Mech. Dev.* **2008**, *125*(5–6), 475.
- [33] K. Nakamoto, *Infrared and Raman Spectra of Inorganic and Coordination Compounds*, Wiley Interscience, New York, NY, USA **1970**.
- [34] L. H. Abdel-Rahman, A. M. Abu-Dief, M. O. Aboelez, A. A. H. Abdel-Mawgoud, *J. Photochem. Photobiol. B* **2017**, *170*, 271.
- [35] S. I. Al-Saedi, L. H. Abdel-Rahman, A. M. Abu-Dief, S. M. Abdel-Fatah, T. M. Alotaibi, A. M. Alsahme, A. Nafady, *Catalysts* **2018**, *8*, 452.
- [36] M. N. Uddin, Z. A. Siddique, N. Mase, M. Uzzaman, W. Shumi, *Appl. Organomet. Chem.* **2019**, *33*, e4876.
- [37] A. M. Abu-Dief, H. M. El-Sagher, M. R. Shehata, *Appl. Organomet. Chem.* **2019**, *33*, e4943.
- [38] A. M. Abu-Dief, L. H. Abdel-Rahman, A. A. Abdelhamid, A. A. Marzouk, M. R. Shehata, M. A. Bakheet, O. A. Almaghrabi, A. Nafady, *Spectrochimica Acta Part a: Mol. And Biomol. Spect.* **2020**, *228*, 117700.
- [39] M. N. Uddin, D. A. Chowdhury, M. M. Rony, M. E. Halim, *Modern Chem.* **2014**, *2*(2), 6.
- [40] M. N. Uddin, D. A. Chowdhury, N. Mase, M. F. Rashid, M. Uzzaman, A. Ahsan, N. M. Shah, *J. Coord. Chem.* **2018**, *71*, 3874. <https://doi.org/10.1080/00958972.2018.1533125>
- [41] J. Aihara, *J. Phys. Chem. A* **1999**, *103*, 7487.
- [42] D. E. Manolopoulos, J. C. May, S. E. Down, *ChemPhysLett* **1991**, *181*, 105.
- [43] L. Ferreira, R. dos Santos, G. Oliva, A. Andricopulo, *Molecules* **2015**, *20*, 13384.
- [44] R. C. Wade, P. J. Goodford, *Prog. Clin. Biol. Res.* **1989**, *289*, 433.
- [45] A. Gleich, B. Kaiser, W. Honscha, H. Fuhrmann, A. Schoeniger, *Cytotechnology* **2019**, *71*, 231.
- [46] M. C. Sanguinetti, M. Tristani-Firouzi, *Nature* **2006**, *440*, 463.

SUPPORTING INFORMATION

Additional supporting information may be found online in the Supporting Information section at the end of this article.

How to cite this article: Uddin MN, Amin MS, Rahman MS, et al. Titanium (IV) complexes of some tetra-dentate symmetrical bis-Schiff bases of 1,6-hexanediamine: Synthesis, characterization, and in silico prediction of potential inhibitor against coronavirus (SARS-CoV-2). *Appl Organomet Chem.* 2021;35:e6067. <https://doi.org/10.1002/aoc.6067>